

# The $\kappa$ - $\mu$ Distribution and the $\eta$ - $\mu$ Distribution

**Michel Daoud Yacoub**

School of Electrical and Computer Engineering, Department of Communications  
University of Campinas  
CP 6101, 13083-852 Campinas, SP, Brazil  
E-mail: michel@decom.fee.unicamp.br

---

## Abstract

This paper presents two general fading distributions, the  $\kappa$ - $\mu$  distribution and the  $\eta$ - $\mu$  distribution, for which fading models are proposed. These distributions are fully characterized in terms of measurable physical parameters. The  $\kappa$ - $\mu$  distribution includes the Rice (Nakagami- $n$ ), the Nakagami- $m$ , the Rayleigh, and the One-Sided Gaussian distributions as special cases. The  $\eta$ - $\mu$  distribution includes the Hoyt (Nakagami- $q$ ), the Nakagami- $m$ , the Rayleigh, and the One-Sided Gaussian distributions as special cases. Field measurement campaigns were used to validate these distributions. It was observed that their fit to experimental data outperformed that provided by the widely known fading distributions, such as the Rayleigh, Rice, and Nakagami- $m$ . In particular, the  $\kappa$ - $\mu$  distribution is better suited for line-of-sight applications, whereas the  $\eta$ - $\mu$  distribution gives better results for non-line-of-sight applications.

Keywords: Fading channels; Gaussian distribution; Rayleigh distributions; Nakagami- $m$  distribution; Rice distribution; Hoyt distribution; Nakagami- $q$  distribution; probability

## 1. Introduction

The propagation of energy in a mobile radio environment is characterized by incident waves interacting with surface irregularities via diffraction, scattering, reflection, and absorption. The interaction of the wave with the physical structures generates a continuous distribution of partial waves [1], with these waves showing amplitudes and phases varying according to the physical properties of the surface. The propagated signal then reaches the receiver through multiple paths, and the result is a combined signal that fades rapidly, characterizing the short-term fading. For surfaces assumed to be of the Gaussian-random rough type, universal statistical laws can be derived in a parameterized form [1].

A great number of distributions exist that well describe the statistics of the mobile radio signal. The long-term signal variation is well characterized by the lognormal distribution, whereas the short-term signal variation is described by several other distributions, such as the Rayleigh, Rice (Nakagami- $n$ ), Nakagami- $m$ , Hoyt (Nakagami- $q$ ), and Weibull distributions. Among the short-term distributions, the Nakagami- $m$  distribution has been given special attention for its ease of manipulation and wide range of applicability [2]. Although, *in general*, it has been found that the fading statistics of the mobile radio channel may well be characterized by the Nakagami- $m$  distribution, situations are easily found for which other distributions, such as the Rice and Weibull distributions, yield better results [3, 4]. More importantly, situations are encountered for which *no distributions* seem to adequately fit experimental data, though one or another may yield a moderate fit. Some

researches [4] even question the use of the Nakagami- $m$  distribution, because its tail does not seem to yield a good fit to experimental data, a better fit being found around the mean or median.

The well-known fading distributions have been derived assuming a homogeneous, diffuse, scattering field, resulting from randomly distributed point scatterers. With such an assumption, the central-limit theorem leads to complex Gaussian processes, with in-phase and quadrature Gaussian-distributed variables having zero means and equal standard deviations. The assumption of a homogeneous diffuse scattering field is certainly an approximation, because the surfaces are spatially correlated, characterizing a non-homogeneous environment [1]. In [5] (and also in [6]), a generalized form for Rice (Nakagami- $n$ ) distributions and another for Hoyt (Nakagami- $q$ ) distributions were presented. These new forms were respectively named the Generalized  $n$ -distribution and the Generalized  $q$ -distribution, and were obtained by considering the summation of squares of the respective independent variables. These distributions have the functional structure of that of the non-central chi-square distribution (in which the degree of freedom is made continuous) and that of the sum of two gamma distributions (or, equivalently, the sum of two central chi-square distributions in which the degree of freedom is made continuous), already presented before in the literature. (For instance, the first one was shown in [7, 8] and also in [9]. The second one was given in [10].) We note, however, that such generalizations were purely connected with a mathematical problem, and did not concern the physical phenomena involved.

The aim of this paper is to propose a general physical fading model, and to describe, parameterize, and fully characterize the corresponding signal in terms of measurable physical parameters. Two fading distributions, the  $\kappa$ - $\mu$  distribution and the  $\eta$ - $\mu$  distribution, are then presented, which have functional similarities to those generalized forms already mentioned. Nonetheless, there is a remarkable difference in the admissible range of one of the parameters. Whereas in the Generalized  $n$ -distribution and in the Generalized  $q$ -distribution, a parameter named  $n$  is permitted "to take any positive number not less than unity at least" [5, 6], the equivalent parameter in the  $\kappa$ - $\mu$  distribution and in the  $\eta$ - $\mu$  distribution (a parameter named  $\mu$ ) may assume any positive value. The  $\kappa$ - $\mu$  distribution includes the Rice (Nakagami- $n$ ) and the Nakagami- $m$  distributions as special cases. The  $\eta$ - $\mu$  distribution includes the Hoyt (Nakagami- $q$ ) and the Nakagami- $m$  distributions as special cases. Therefore, in both fading distributions, the One-Sided Gaussian and the Rayleigh distributions also constitute special cases. In addition to the characterization of the distributions in terms of measurable physical fading parameters, as well as the allowance for a more comprehensive range of values of their parameters, this paper provides several other contributions, including: (i) attainment of exact and closed-form moment-based estimators for the parameters; (ii) a proposal for practical procedures to apply the distributions; (iii) the derivation of exact and closed-form formulas for the distributions at the limiting values of the parameters; (iv) a portrayal of important attributes of the distributions, envisaged as they are plotted in what here is named "the fading plane;" and (v) validation of the distributions through field measurements. It has been observed that the fit of these distributions to experimental data outperforms that provided by the widely known fading distributions, such as Rice and Nakagami- $m$ . Moreover, in these measurements, it was always possible to adequately fit experimental data through either the  $\kappa$ - $\mu$  distribution or the  $\eta$ - $\mu$  distribution. As shall be seen later in this paper, the question raised in [4] concerning the inadequacy of the tails of some distributions to fit experimental data is notably less critical in these distributions. This work gathers, develops, enhances, and extends the results from [11, 12, 13]. (Throughout the text,  $E(\bullet)$  and  $V(\bullet)$  are used to denote the expectation and variance operators.)

## 2. The $\kappa$ - $\mu$ Distribution

The  $\kappa$ - $\mu$  distribution is a general fading distribution that can be used to represent the small-scale variation of the fading signal in a *line-of-sight condition*. For a fading signal with envelope,  $R$ , and normalized envelope,  $P = R/\hat{r}$ , with  $\hat{r} = \sqrt{E(R^2)}$  being the *rms* value of  $R$ , the  $\kappa$ - $\mu$  envelope probability density function,  $f_P(\rho)$ , is written as

$$f_P(\rho) = \frac{2\mu(1+\kappa)^{\frac{\mu+1}{2}}}{\kappa^{\frac{\mu-1}{2}} \exp(\mu\kappa)} \rho^\mu \exp[-\mu(1+\kappa)\rho^2] I_{\mu-1} \left[ 2\mu\sqrt{\kappa(1+\kappa)}\rho \right], \quad (1)$$

where  $\kappa > 0$  is the ratio between the total power of the dominant components and the total power of the scattered waves,  $\mu > 0$  is

given by  $\mu = \frac{E^2(R^2)}{V(R^2)} \frac{1+2\kappa}{(1+\kappa)^2}$  (or, equivalently,

$$\mu = \frac{1}{V(P^2)} \frac{1+2\kappa}{(1+\kappa)^2}), \text{ and } I_\nu(\bullet) \text{ is the modified Bessel function of}$$

the first kind and order  $\nu$  [14, Equation 9.6.20]. For a fading signal with power  $W = R^2$  and normalized power  $\Omega = W/\bar{w}$ , where  $\bar{w} = E(W)$ , the  $\kappa$ - $\mu$  power probability density function,  $f_\Omega(\omega)$ , is given by

$$f_\Omega(\omega) = \frac{\mu(1+\kappa)^{\frac{\mu+1}{2}}}{\kappa^{\frac{\mu-1}{2}} \exp(\mu\kappa)} \omega^{\frac{\mu-1}{2}} \exp[-\mu(1+\kappa)\omega] I_{\mu-1} \left[ 2\mu\sqrt{\kappa(1+\kappa)}\omega \right]. \quad (2)$$

In particular, we may also write  $\mu = \frac{E^2(W)}{V(W)} \frac{1+2\kappa}{(1+\kappa)^2}$  (or, equivalently,

$$\mu = \frac{1}{V(\Omega)} \frac{1+2\kappa}{(1+\kappa)^2}). \text{ The } \kappa\text{-}\mu \text{ envelope probability distribu-}$$

tion function,  $F_P(\rho)$ , is obtained in closed form as

$$F_P(\rho) = 1 - Q_\mu \left[ \sqrt{2\kappa\mu}, \sqrt{2(1+\kappa)\mu}\rho \right], \quad (3)$$

where

$$Q_\nu(a, b) = \frac{1}{a^{\nu-1}} \int_b^\infty x^\nu \exp\left(-\frac{x^2+a^2}{2}\right) I_{\nu-1}(ax) dx \quad (4)$$

is the generalized Marcum  $Q$  function [8]. The  $j$ th moment,  $E(P^j)$ , of  $P$  is found in a closed-form formula as

$$E(P^j) = \frac{\Gamma(\mu + j/2) \exp(-\kappa\mu)}{\Gamma(\mu) [(1+\kappa)\mu]^{j/2}} {}_1F_1(\mu + j/2; \mu; \kappa\mu), \quad (5)$$

where  $\Gamma(\bullet)$  is the Gamma function [14, Equation 6.1.1] and  ${}_1F_1(\bullet; \bullet; \bullet)$  is the confluent hypergeometric function [14, Equation 13.1.2]. Of course,  $E(R^k) = \hat{r}^k E(P^k)$ . Figure 1, for a fixed  $\mu$  ( $\mu = 0.5$ ) and varying  $\kappa$ , and Figure 2, for a fixed  $\kappa$  ( $\kappa = 1$ ) and varying  $\mu$ , show the various shapes of the  $\kappa$ - $\mu$  probability density function,  $f_P(\rho)$ . In Figure 1, the case in which  $\kappa = 0$  and  $\mu = 0.5$  coincides with that for Nakagami- $m$  with  $m = 0.5$ , where  $m$  is the Nakagami- $m$  parameter. In Figure 2, the case in which  $\mu = 1$  and  $\kappa = 1$  coincides with that for Rice with  $k = 1$ , where  $k$  is the Rice parameter.

### 2.1 Physical Model for the $\kappa$ - $\mu$ Distribution

The fading model for the  $\kappa$ - $\mu$  distribution considers a signal composed of clusters of multipath waves, propagating in a non-homogeneous environment. Within any one cluster, the phases of

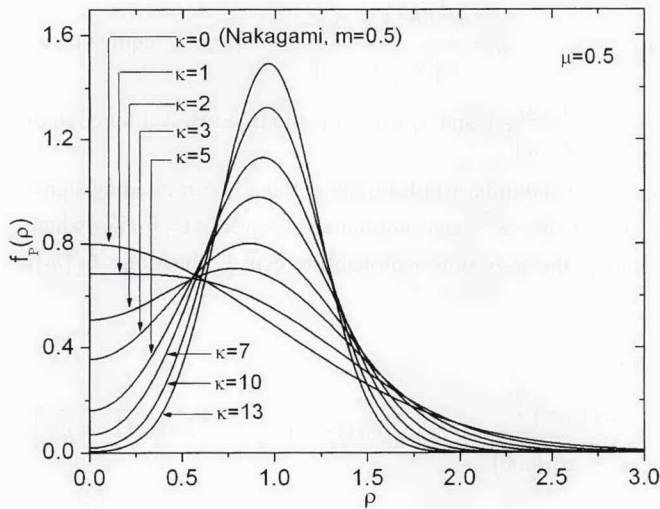


Figure 1. The  $\kappa$ - $\mu$  probability density function for a fixed  $\mu$  ( $\mu = 0.5$ ).

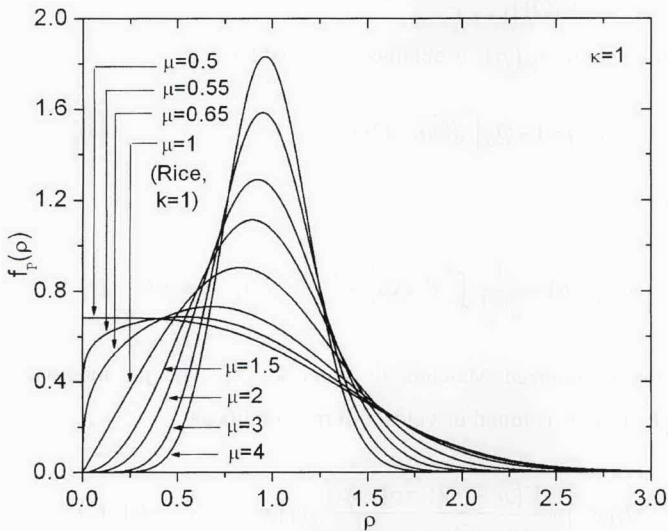


Figure 2. The  $\kappa$ - $\mu$  probability density function for a fixed  $\kappa$  ( $\kappa = 1.0$ ).

the scattered waves are random and have similar delay times, with delay-time spreads of different clusters being relatively large. The clusters of multipath waves are assumed to have scattered waves with identical powers, but within each cluster a dominant component is found, which presents an arbitrary power.

## 2.2 Derivation of the $\kappa$ - $\mu$ Distribution

Given the physical model for the  $\kappa$ - $\mu$  distribution, the envelope,  $R$ , can be written in terms of the in-phase and quadrature components of the fading signal as

$$R^2 = \sum_{i=1}^n (X_i + p_i)^2 + \sum_{i=1}^n (Y_i + q_i)^2, \quad (6)$$

where  $X_i$  and  $Y_i$  are mutually independent Gaussian processes with  $E(X_i) = E(Y_i) = 0$ ,  $E(X_i^2) = E(Y_i^2) = \sigma^2$ ;  $p_i$  and  $q_i$  are

respectively the mean values of the in-phase and quadrature components of the multipath waves of cluster  $i$ ; and  $n$  is the number of clusters of multipath. Now, we form the process  $R_i^2 = (X_i + p_i)^2 + (Y_i + q_i)^2$ , so that  $R^2 = \sum_{i=1}^n R_i^2$ . In the same way, we may write  $W = \sum_{i=1}^n W_i$ , where  $W = R^2$  and  $W_i = R_i^2$ . We proceed to find the probability density function,  $f_{W_i}(w_i)$ , of  $W_i$ . This can be carried out by following the standard procedure, so that

$$f_{W_i}(w_i) = \frac{1}{2\sigma^2} \exp\left(-\frac{w_i + d_i^2}{2\sigma^2}\right) I_0\left(\frac{d_i \sqrt{w_i}}{\sigma^2}\right),$$

where  $d_i^2 = p_i^2 + q_i^2$ , and  $I_0(\cdot)$  is the modified Bessel function of the first kind and order zero [14, Equation 9.6.16].

The Laplace transform,  $L[f_{W_i}(w_i)]$  of  $f_{W_i}(w_i)$ , is found to be [14, Equation 29.3.81]

$$L[f_{W_i}(w_i)] = \frac{1}{1 + 2s\sigma^2} \exp\left(-\frac{s d_i^2}{1 + 2s\sigma^2}\right),$$

where  $s$  is the complex frequency (the Laplace variable). Knowing that the  $W_i$ ,  $i = 1, 2, \dots, n$ , are independent random variables, the Laplace transform,  $L[f_W(w)]$ , of  $f_W(w)$  is found to be

$$L[f_W(w)] = \frac{1}{(1 + 2s\sigma^2)^n} \exp\left(-\frac{s d^2}{1 + 2s\sigma^2}\right),$$

where  $d^2 = \sum_{i=1}^n d_i^2$ . The inverse of this is given by [14, Equation 29.3.81]

$$f_W(w) = \frac{1}{2\sigma^2} \left(\frac{w}{d^2}\right)^{\frac{n-1}{2}} \exp\left(-\frac{w + d^2}{2\sigma^2}\right) I_{n-1}\left(\frac{d \sqrt{w}}{\sigma^2}\right). \quad (7)$$

It can be seen that  $\hat{r}^2 = E(R^2) = \bar{w} = E(W) = 2n\sigma^2 + d^2$ , and that

$$E(R^4) = E(W^2) = 4n\sigma^4 + 4\sigma^2 d^2 + (2n\sigma^2 + d^2)^2. \quad \text{Therefore,}$$

$V(R^2) = V(W) = 4n\sigma^4 + 4\sigma^2 d^2$ . We define  $\kappa = \frac{d^2}{2n\sigma^2}$  as the ratio between the total power of the dominant components and the total power of the scattered waves. Then,

$$\frac{E^2(R^2)}{V(R^2)} = \frac{E^2(W)}{V(W)} = n \frac{(1 + \kappa)^2}{(1 + 2\kappa)}. \quad (8)$$

From Equation (8), note that  $n$  may be totally expressed in terms of physical parameters, such as mean-squared value of the power, the variance of the power, and the ratio of the total power of the dominant components and the total power of the scattered waves of the fading signal. Note also that whereas these physical parameters are of a continuous nature,  $n$  is of a discrete nature. It is plausible to presume that if these parameters are to be obtained by field measurements, their ratios, as defined in Equation (8), will certainly lead to figures that may depart from the exact  $n$ . Several reasons

exist for this. One of them – probably the most meaningful one – is that although the model proposed here is general, it is in fact an approximate solution to the so-called random phase problem, as are all the other well-known fading models approximate solutions to the random phase problem.

The limitation of the model can be made less stringent by defining  $\mu$  to be

$$\mu = \frac{1}{V(P^2)} \frac{1+2\kappa}{(1+\kappa)^2} = \frac{1}{V(\Omega)} \frac{1+2\kappa}{(1+\kappa)^2}, \quad (9)$$

with  $\mu$  being the *real* extension of  $n$ , and  $V(P^2) = V(R^2)/E^2(R^2)$ ,  $V(\Omega) = V(W)/E^2(W)$ . Non-integer values of the parameter  $\mu$  may account for a) non-zero correlation among the clusters of multipath components; b) non-zero correlation between the in-phase and quadrature components within each cluster; c) the non-Gaussian nature of the in-phase and quadrature components of each cluster of the fading signal, among other factors. Non-integer values of clusters have been found in practice, and are extensively reported in the literature. (See, for instance, [15], and the references therein.) And, of course, scattering occurs continuously throughout the surface, and not at discrete points [1]. Using the definitions and the considerations as given above, and by means of a transformation of variables and a series of algebraic manipulations, the  $\kappa$ - $\mu$  power probability density function can be written from Equation (7) as

$$\bar{w}f_W(w) = \frac{\mu(1+\kappa)^{\frac{\mu+1}{2}}}{\kappa^{\frac{\mu-1}{2}} \exp(\mu\kappa)} \left(\frac{w}{\bar{w}}\right)^{\frac{\mu-1}{2}} \exp\left(-\frac{\mu(1+\kappa)w}{\bar{w}}\right) I_{\mu-1}\left(2\mu\sqrt{\frac{\kappa(1+\kappa)w}{\bar{w}}}\right), \quad (10)$$

which, in its normalized version, yields Equation (2). The  $\kappa$ - $\mu$  envelope probability density function can be written from Equation (10) as

$$\hat{r}f_R(r) = \frac{2\mu(1+\kappa)^{\frac{\mu+1}{2}}}{\kappa^{\frac{\mu-1}{2}} \exp(\mu\kappa)} \left(\frac{r}{\hat{r}}\right)^{\mu} \exp\left(-\mu(1+\kappa)\left(\frac{r}{\hat{r}}\right)^2\right) I_{\mu-1}\left(2\mu\sqrt{\frac{\kappa(1+\kappa)r}{\hat{r}}}\right), \quad (11)$$

which, in its normalized version, yields Equation (1).

## 2.3 The $\kappa$ - $\mu$ Distribution and the Other Fading Distributions

The  $\kappa$ - $\mu$  distribution is a general fading distribution that includes the best-known fading distributions, namely the Rice and Nakagami- $m$  distributions. Note that both the Rice and Nakagami- $m$  distributions include the Rayleigh distribution, and, in addition, the Nakagami- $m$  distribution also includes the One-Sided Gaussian distribution. Therefore, these distributions can also be obtained from the  $\kappa$ - $\mu$  distribution.

### 2.3.1 Rice and Rayleigh

The Rice distribution describes a fading signal with one cluster of multipath waves in which one specular component predominates over the scattered waves. Therefore, it can be obtained from the  $\kappa$ - $\mu$  distribution by setting  $\mu=1$  in Equation (1) or, equivalently, in Equation (11). In this case, the parameter  $\kappa$  coincides with the well-known Rice parameter  $k$ . From the Rice distribution, by setting  $\kappa=k=0$  (therefore,  $\mu=1$  and  $\kappa \rightarrow 0$  in the  $\kappa$ - $\mu$  distribution), the Rayleigh distribution can be obtained in an exact manner.

### 2.3.2 Nakagami- $m$ , Rayleigh, and One-Sided Gaussian

The Nakagami- $m$  signal can be understood to be composed of clusters of multipath waves with no dominant components within any cluster. Therefore, by setting  $\kappa=0$  in the  $\kappa$ - $\mu$  distribution, it should be possible to obtain the Nakagami- $m$  distribution. However, we note that apart from the case  $\mu=1$ , which has been explored in the previous subsection, the introduction of  $\kappa=0$  in the  $\kappa$ - $\mu$  distribution leads to indeterminacy (zero divided by zero). Appendix A shows that in the limit as  $\kappa \rightarrow 0$ , the  $\kappa$ - $\mu$  distribution deteriorates into the *exact* Nakagami- $m$  density function. In this case, the parameter  $\mu$  coincides with the well-known Nakagami parameter  $m$ . Now, setting  $\mu=m=1$  in the Nakagami- $m$  distribution (therefore,  $\mu=1$  and  $\kappa \rightarrow 0$  in the  $\kappa$ - $\mu$  distribution), the Rayleigh distribution can be obtained in an exact manner. In the same way, by setting  $\mu=m=0.5$  in the Nakagami- $m$  distribution (therefore,  $\mu=0.5$  and  $\kappa \rightarrow 0$  in the  $\kappa$ - $\mu$  distribution), the One-Sided Gaussian distribution can be obtained in an exact manner.

## 2.4 Estimators for the Parameters

Moment-based estimators for the parameters  $\kappa$  and  $\mu$  can be obtained as follows. Replacing Equation (9) in Equation (5) for  $j=6$ , and after algebraic manipulations,  $\kappa$  is found to be

$$\kappa^{-1} = \frac{\sqrt{2} [E(\rho^4) - 1]}{\sqrt{2E^2(\rho^4) - E(\rho^4) - E(\rho^6)}} - 2. \quad (12)$$

The parameter  $\mu$  is obtained from Equation (9).

## 2.5 Application of the $\kappa$ - $\mu$ Distribution

As implied in its name, the  $\kappa$ - $\mu$  distribution is based on two parameters,  $\kappa$  and  $\mu$ . Therefore, its use requires the estimation of these parameters. Alternatively, the following procedure may be carried out in order to use it. From Equation (9), it can be seen that the two parameters,  $\kappa$  and  $\mu$ , can be expressed in terms of the normalized variance of the power of the fading signal, which is usually defined as  $m$ . In other words,

$$m = \frac{\mu(1+\kappa)^2}{1+2\kappa}. \quad (13)$$

For a given  $m$ , the parameters  $\kappa$  and  $\mu$  are chosen to yield the best fit. On the other hand, note that for a given  $m$ , the parameter  $\mu$  will lie within the range  $m$  and 0, obtained for  $\kappa = 0$  and  $\kappa \rightarrow \infty$ , respectively. Therefore, for a given  $m$ ,

$$0 \leq \mu \leq m. \quad (14)$$

The parameter  $\mu$  is then chosen within the range of Equation (14). Given that  $\mu$  has been chosen, then  $\kappa$  is calculated from Equation (13) to be

$$\kappa = \frac{m}{\mu} - 1 + \sqrt{\frac{m}{\mu} \left( \frac{m}{\mu} - 1 \right)}. \quad (15)$$

## 2.6 The $\kappa$ - $\mu$ Distribution for a Fixed $m$

Equation (13) shows that for a given  $m$ , an infinite number of curves of the  $\kappa$ - $\mu$  distribution can be found that present the same Nakagami- $m$  parameter, conditioned on the fact that the constraints of Equations (14) and (15) are satisfied. The Nakagami- $m$  curve is obtained for  $\kappa \rightarrow 0$ , in which case  $\mu = m$ . The Rice curve is obtained for  $\mu = 1$ , in which case  $\kappa = k$ . Given that  $\mu > 0$  and  $\kappa > 0$ , and that a relationship among  $\kappa$ ,  $\mu$ , and  $m$  is found through Equation (13), for a fixed  $m$ , as  $\mu \rightarrow 0$  then  $\kappa \rightarrow \infty$ . In such a case, it can be shown that (see Appendix A)

$$f_p(\rho) = \frac{4m I_1(4m\rho)}{\exp[2m(1+\rho^2)]} + \left[ 1 - \frac{\sqrt{2m\pi}}{\exp(m)} I_{0.5}(m) \right] \delta(\rho), \quad (16)$$

where  $\delta(\rho)$  is the Dirac delta function. Figures 3 and 4, respectively, depict a sample of the various shapes of the  $\kappa$ - $\mu$  probability density function,  $f_p(\rho)$ , and the probability distribution function,  $F_p(\rho)$ , as functions of the normalized envelope,  $\rho$ , for the same Nakagami parameter,  $m = 1.25$ . The curves for which  $\mu \rightarrow 0$ , or equivalently  $\kappa \rightarrow \infty$ , appear indicated by  $\mu = 0$ , and are obtained by means of Equation (16). In Figure 3, as  $\mu$  decreases, an impulse tends to occur at the origin. In the limit as  $\mu \rightarrow 0$ , an impulse does occur, the amplitude of which is given by the right-hand side of Equation (16). Note in Figure 4 that departing from the condition  $\mu = m$ , the curves for decreasing  $\mu$  are sequentially found above that for  $\mu = m$ . It can be seen that although the normalized variance (parameter  $m$ ) is kept constant for each figure, the curves are substantially different from each other. This is particularly relevant for the distribution function, in which case the lower tail of the distribution may yield differences of some orders of magnitude in the probability. This feature renders the  $\kappa$ - $\mu$  distribution very flexible, and this flexibility can be used in order to adjust the curves to practical data.

## 2.7 Sum of $\kappa$ - $\mu$ Variates

From the definition of the  $\kappa$ - $\mu$  distribution, it is easy to see that the sum of  $M$  independent identically distributed (IID)  $\kappa$ - $\mu$  power variates is also  $\kappa$ - $\mu$  distributed, with parameters  $\kappa$  and  $\mu M$ . Now, the sum of  $M$  independent identically distributed  $\kappa$ - $\mu$  envelope variates may be well approximated by another  $\kappa$ - $\mu$

distribution, the parameters of which are estimated accordingly. The procedure for obtaining these parameters follows that given in [16], where it was shown that the  $\kappa$ - $\mu$  distribution can be used in order to approximate the distribution of the sum of Rice (and also Nakagami- $m$ ) variates. In [16], it was demonstrated that exact and approximate curves are almost indistinguishable from each other. The distribution of the sum of independent non-identically distributed  $\kappa$ - $\mu$  variates (power or envelope) may also be approximated by a  $\kappa$ - $\mu$  distribution, although in this case, the resulting curves are not as accurate as for the independent identically distributed case.

## 3. The $\eta$ - $\mu$ Distribution

The  $\eta$ - $\mu$  distribution is a general fading distribution that can be used to better represent the small-scale variation of the fading signal in a *non-line-of-sight* condition. It may appear in two differ-

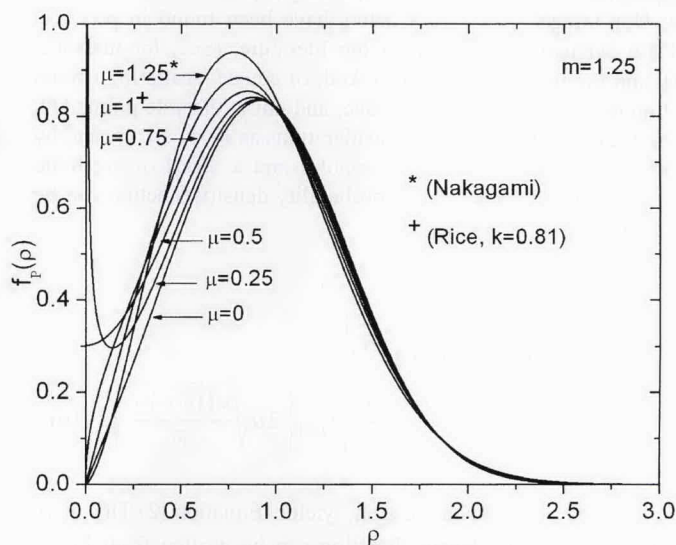


Figure 3. The  $\kappa$ - $\mu$  probability density function for the same Nakagami parameter  $m$  ( $m = 1.25$ ).

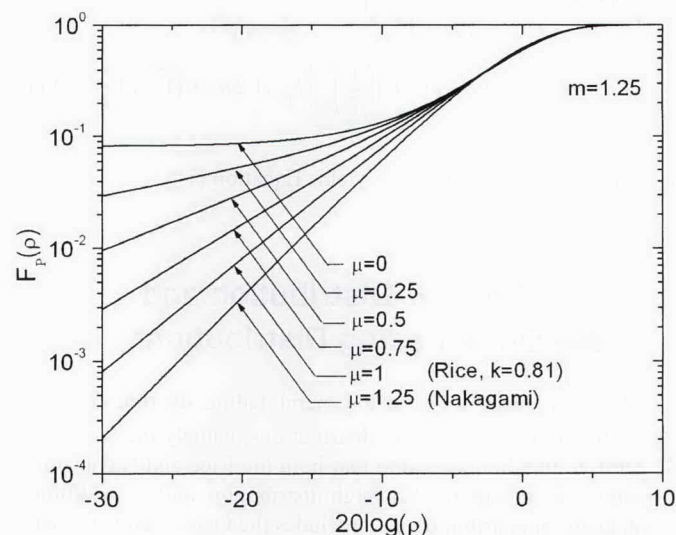


Figure 4. The  $\kappa$ - $\mu$  probability distribution function for the same Nakagami parameter  $m$  ( $m = 1.25$ ).

ent formats, for which two corresponding physical models are encountered. However, in mathematical terms, one format can be obtained from another by the relation  $\eta_{\text{Format2}} = \frac{1 - \eta_{\text{Format1}}}{1 + \eta_{\text{Format1}}}$  or, equivalently,  $\eta_{\text{Format1}} = \frac{1 - \eta_{\text{Format2}}}{1 + \eta_{\text{Format2}}}$ , where  $0 < \eta_{\text{Format1}} < \infty$  is the parameter  $\eta$  in Format 1, and  $-1 < \eta_{\text{Format2}} < 1$  is the parameter  $\eta$  in Format 2. For convenience, and in order to simplify the notation, we shall use  $\eta$  in both cases, bearing in mind that they represent different physical phenomena and their ranges are different. The notation is further simplified if we define two other parameters, namely  $h$  and  $H$ , which are functions of  $\eta$ . Therefore, these parameters assume different meanings and values for the two different formats. The convenience of using these two parameters is to have a unified representation for both formats.

For a fading signal with envelope  $R$  and normalized envelope  $P = R/\hat{r}$ ,  $\hat{r} = \sqrt{E(R^2)}$  being the *rms* value of  $R$ , the  $\eta$ - $\mu$  envelope probability density function,  $f_P(\rho)$ , is written as

$$f_P(\rho) = \frac{4\sqrt{\pi}\mu^{\mu+\frac{1}{2}}h^\mu}{\Gamma(\mu)H^{\mu-\frac{1}{2}}} \rho^{2\mu} \exp(-2\mu h\rho^2) I_{\mu-\frac{1}{2}}(2\mu H\rho^2), \quad (17)$$

where  $h$  and  $H$  will be defined next for the two different formats;

$$\mu > 0 \text{ is given by } \mu = \frac{E^2(R^2)}{2V(R^2)} \left[ 1 + \left( \frac{H}{h} \right)^2 \right] \quad (\text{or equivalently,}$$

$$\mu = \frac{1}{2V(P^2)} \left[ 1 + \left( \frac{H}{h} \right)^2 \right]; \Gamma(\cdot) \text{ is the Gamma function [14, Equation 6.1.1]; and } I_\nu(\cdot) \text{ is the modified Bessel function of the first kind and order } \nu \text{ [14, Equation 9.6.20].}$$

For a fading signal with power  $W = R^2$  and normalized power  $\Omega = W/\bar{w}$ , where  $\bar{w} = E(W)$ , the  $\eta$ - $\mu$  power probability density function,  $f_\Omega(\omega)$ , is given by

$$f_\Omega(\omega) = \frac{2\sqrt{\pi}\mu^{\mu+\frac{1}{2}}h^\mu}{\Gamma(\mu)H^{\mu-\frac{1}{2}}} \omega^{\mu-\frac{1}{2}} \exp(-2\mu h\omega) I_{\mu-\frac{1}{2}}(2\mu H\omega). \quad (18)$$

In particular, we may also write  $\mu = \frac{E^2(W)}{2V(W)} \left[ 1 + \left( \frac{H}{h} \right)^2 \right]$  (or

equivalently,  $\mu = \frac{1}{2V(\Omega)} \left[ 1 + \left( \frac{H}{h} \right)^2 \right]$ ). The  $\eta$ - $\mu$  envelope probability distribution function,  $F_P(\rho)$ , is written as

$$F_P(\rho) = 1 - Y_\mu \left( \frac{H}{h}, \sqrt{2h\mu} \rho \right), \quad (19)$$

where, for convenience, the following function is defined:

$$Y_\nu(a, b) = \frac{2^{2-\nu} \sqrt{\pi} (1-a^2)^\nu}{a^{\nu-\frac{1}{2}} \Gamma(\nu)} \int_b^\infty x^{2\nu} \exp(-x^2) I_{\nu-\frac{1}{2}}(ax^2) dx, \quad (20)$$

with  $-1 < a < 1$  and  $b \geq 0$ . (Some properties of  $Y_\nu(a, b)$  are shown in Appendix C.) The  $j$ th moment,  $E(P^j)$ , of  $P$  is found in a closed-form formula as

$$E(P^j) = \frac{\Gamma(2\mu + j/2)}{h^{\mu+j/2} (2\mu)^{j/2} \Gamma(2\mu)} {}_2F_1 \left[ \mu + \frac{j}{4} + \frac{1}{2}, \mu + \frac{j}{4}; \mu + \frac{1}{2}; \left( \frac{H}{h} \right)^2 \right], \quad (21)$$

where  ${}_2F_1(\cdot, \cdot; \cdot; \cdot)$  is the Gauss hypergeometric function [14, Equation 15.1.1]. Of course,  $E(R^j) = \hat{r}^j E(P^j)$ .

Figure 5, for a fixed  $\mu$  ( $\mu = 0.6$ ) and varying  $\eta$ , and Figure 6, for a fixed  $\eta$  ( $\eta = 0.5$ ) and varying  $\mu$ , show the various shapes of the  $\eta$ - $\mu$  probability density function,  $f_P(\rho)$ . In both

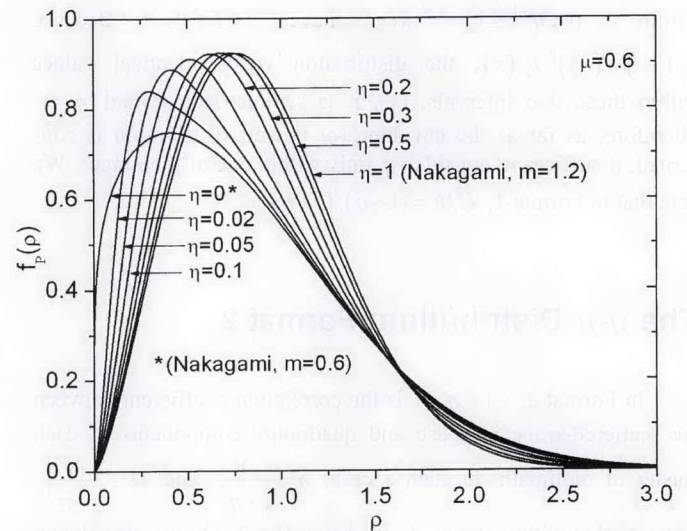


Figure 5. The  $\eta$ - $\mu$  probability density function for a fixed  $\mu$  ( $\mu = 0.6$ ).

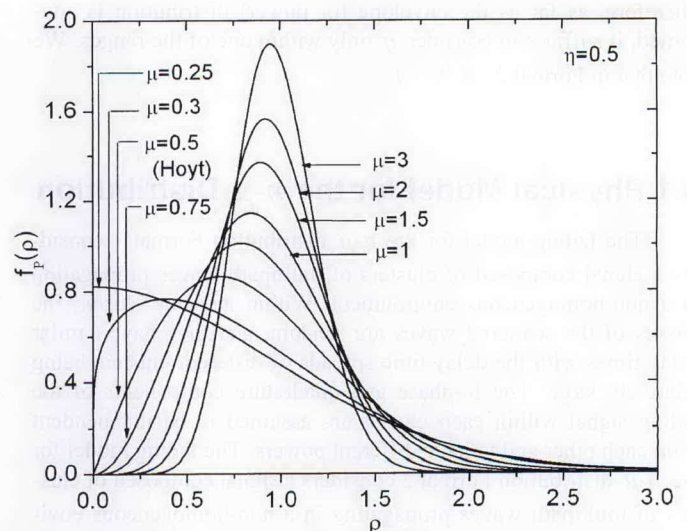


Figure 6. The  $\eta$ - $\mu$  probability density function for a fixed  $\eta$  ( $\eta = 0.5$ ).

figures, and in all of the others, the values of  $\eta$  are for Format 1. In Figure 5, the case in which  $\eta = 0$  ( $\mu = 0.6$ ) coincides with that for Nakagami- $m$  with  $m = 0.6$ , where  $m$  is the Nakagami parameter. Still in Figure 5, the case in which  $\eta = 1$  ( $\mu = 0.6$ ) coincides with that for Nakagami- $m$  with  $m = 1.2$ . In Figure 6, the case in which  $\mu = 0.5$  ( $\eta = 0.5$ ) coincides with that for Hoyt with  $b = 1/3$ , where  $b$  is the Hoyt parameter, or equivalently with that of Nakagami- $q$  with  $q^2 = 0.5$ . The reader is referred to Appendix B for the extended forms of these two formats, where they are written in terms of the parameters  $\eta$  and  $\mu$ .

### The $\eta$ - $\mu$ Distribution: Format 1

In Format 1,  $0 < \eta < \infty$  is the scattered-wave power ratio between the in-phase and quadrature components of each cluster of multipath. In such a case,  $h = \frac{2+\eta^{-1}+\eta}{4}$  and  $H = \frac{\eta^{-1}-\eta}{4}$ . We note that within  $0 < \eta \leq 1$ , we have  $H \geq 0$ . On the other hand, within  $0 < \eta^{-1} \leq 1$ , we have  $H \leq 0$ . Because  $I_\nu(-z) = (-1)^\nu I_\nu(z)$ , the distribution yields identical values within these two intervals, i.e., it is symmetrical around  $\eta = 1$ . Therefore, as far as the envelope (or power) distribution is concerned, it suffices to consider  $\eta$  only within one of the ranges. We note that in Format 1,  $H/h = (1-\eta)/(1+\eta)$ .

### The $\eta$ - $\mu$ Distribution: Format 2

In Format 2,  $-1 < \eta < 1$  is the correlation coefficient between the scattered-wave in-phase and quadrature components of each cluster of multipath. In such a case,  $h = \frac{1}{1-\eta^2}$  and  $H = \frac{\eta}{1-\eta^2}$ . We note that within  $0 \leq \eta < 1$ , we have  $H \geq 0$ . On the other hand, within  $-1 < \eta \leq 0$ , we have  $H \leq 0$ . Because  $I_\nu(-z) = (-1)^\nu I_\nu(z)$ , the distribution yields identical values within these two intervals, i.e. it is symmetrical around  $\eta = 0$ . Therefore, as far as the envelope (or power) distribution is concerned, it suffices to consider  $\eta$  only within one of the ranges. We note that in Format 2,  $H/h = \eta$ .

### 3.1 Physical Model for the $\eta$ - $\mu$ Distribution

The fading model for the  $\eta$ - $\mu$  distribution Format 1 considers a signal composed of clusters of multipath waves propagating in a non-homogeneous environment. Within any one cluster, the phases of the scattered waves are random, and they have similar delay times with the delay-time spreads of different clusters being relatively large. The in-phase and quadrature components of the fading signal within each cluster are assumed to be independent from each other and to have different powers. The fading model for the  $\eta$ - $\mu$  distribution Format 2 considers a signal composed of clusters of multipath waves propagating in a non-homogeneous environment. Within any one cluster, the phases of the scattered waves are random, and have similar delay times with delay-time spreads of different clusters being relatively large. The in-phase and quad-

rate components of the fading signal within each cluster are assumed to have identical powers and to be correlated with each other.

### 3.2 Derivation of the $\eta$ - $\mu$ Distribution

Initially, consider the physical model for the  $\eta$ - $\mu$  distribution Format 1. The envelope,  $R$ , can be written in terms of the in-phase and quadrature components of the fading signal as

$$R^2 = \sum_{i=1}^n (X_i^2 + Y_i^2), \quad (22)$$

where  $X_i$  and  $Y_i$  are mutually independent Gaussian processes with  $E(X_i) = E(Y_i) = 0$ ,  $E(X_i^2) = \sigma_X^2$ ,  $E(Y_i^2) = \sigma_Y^2$ , and  $n$  is the number of clusters of multipath. Now, we form the process  $R_i^2 = X_i^2 + Y_i^2$ , so that  $R^2 = \sum_{i=1}^n R_i^2$ . In the same way, we may write  $W = \sum_{i=1}^n W_i$ , where  $W = R^2$  and  $W_i = R_i^2$ . We proceed to find the probability density function,  $f_{W_i}(w_i)$ , of  $W_i$ . This can be carried out by following the standard procedure, so that

$$f_{W_i}(w_i) = \frac{n\sqrt{h}}{\bar{w}} \exp\left(-\frac{nhw_i}{\bar{w}}\right) I_0\left(\frac{nHw_i}{\bar{w}}\right),$$

where  $h$  and  $H$  are as already defined for Format 1,  $\eta = \sigma_X^2/\sigma_Y^2$  is the scattered-wave power ratio between the in-phase and quadrature components of each cluster of multipath,  $I_0(\cdot)$  is the modified Bessel function of the first kind of order zero [14, Equation 9.6.16], and, for convenience, we have defined  $\bar{w}^2 = E(R^2) = nE(R_i^2) = \bar{w} = E(W) = nE(W_i) = n(1+\eta^{-1})\sigma_X^2$ . (Note that  $\bar{w}/n$  is the signal power of one cluster.) Note that  $0 < \eta \leq 1$  defines the region within which  $\sigma_X^2 \leq \sigma_Y^2$ , whereas  $0 < \eta^{-1} \leq 1$  defines the region within which  $\sigma_Y^2 \leq \sigma_X^2$ . The Laplace transform,  $L[f_{W_i}(w_i)]$  of  $f_{W_i}(w_i)$ , is found to be [14, Equation 29.3.60]

$$L[f_{W_i}(w_i)] = \frac{n\sqrt{h}/\bar{w}}{\sqrt{(s+nh/\bar{w})^2 - (nH/\bar{w})^2}}.$$

Knowing that the  $W_i$ ,  $i = 1, 2, \dots, n$ , are independent, the Laplace transform,  $L[f_W(w)]$ , of  $f_W(w)$  is found to be

$$L[f_W(w)] = \left[ \frac{n\sqrt{h}/\bar{w}}{\sqrt{(s+nh/\bar{w})^2 - (nH/\bar{w})^2}} \right]^n,$$

the inverse of which is given by [14, Equation 29.3.60]

$$\bar{w}f_W(w) = \frac{\sqrt{\pi}n^{-\frac{n+1}{2}}h^{\frac{n}{2}}}{(2H)^{\frac{n-1}{2}}\Gamma\left(\frac{n}{2}\right)} \left(\frac{w}{\bar{w}}\right)^{\frac{n-1}{2}} \exp\left(-\frac{nhw}{\bar{w}}\right) I_{\frac{n-1}{2}}\left(\frac{nHw}{\bar{w}}\right). \quad (23)$$

It can be seen that  $\hat{r}^2 = E(R^2) = \bar{w} = E(W) = n(1+\eta)\sigma_Y^2$  and that  $E(R^4) = E(W^2) = [2n(1+\eta^2) + n^2(1+\eta)^2]\sigma_Y^4$ . Therefore,  $Var(R^2) = V(W) = 2n(1+\eta^2)\sigma_Y^4$ . Thus,

$$\frac{E^2(R^2)}{V(R^2)} = \frac{E^2(W)}{V(W)} = \frac{n(1+\eta)^2}{2(1+\eta^2)}. \quad (24)$$

Note from Equation (24) that  $n/2$  may be totally expressed in terms of physical parameters, such as the mean-squared value of the power, the variance of the power, and the power of the in-phase and quadrature components of the fading signal. Note also that whereas these physical parameters are of a continuous nature,  $n/2$  is of a discrete nature (an integer multiple of  $1/2$ ). It is plausible to presume that if these parameters are to be obtained by field measurements, their ratios, as defined in Equation (24), will certainly lead to values that may depart from the exact  $n/2$ . Several reasons exist for this. One of them – probably the most meaningful one – is that although the model proposed here is general, it is in fact an approximate solution to the so-called random-phase problem, as are all the other well-known fading models approximate solutions to the random-phase problem. The limitation of the model can be made less stringent by defining  $\mu$  to be

$$\mu = \frac{1}{2V(P^2)} \left[ 1 + \left( \frac{H}{h} \right)^2 \right] = \frac{1}{2V(\Omega)} \left[ 1 + \left( \frac{H}{h} \right)^2 \right], \quad (25)$$

with  $\mu$  being the *real* extension of  $n/2$ ,  $V(P^2) = V(R^2)/E^2(R^2)$ ,  $V(\Omega) = V(W)/E^2(W)$ , and  $h$  and  $H$  are as defined. Values of  $\mu$  that differ from multiples of  $1/2$  correspond to non-integer values of clusters, and may account for a) nonzero correlation among the clusters of multipath components; b) nonzero correlation between the in-phase and quadrature components within each cluster; and/or c) the non-Gaussian nature of the in-phase and quadrature components of each cluster of the fading signal, among others. Non-integer values of clusters have been found in practice, and are extensively reported in the literature. (See, for instance, [15], and the references therein.) Of course, scattering occurs continuously throughout the surface and not at discrete points [1]. Using the definitions and the considerations as above and some algebraic manipulations, the  $\eta$ - $\mu$  power probability density function can be written from Equation (23) as

$$\bar{w}f_W(w) = \frac{2\sqrt{\pi}\mu^{\mu+1/2}h^\mu}{\Gamma(\mu)H^{\mu-1/2}} \left( \frac{w}{\bar{w}} \right)^{\mu-1/2} \exp\left(-\frac{2\mu hw}{\bar{w}}\right) I_{\mu-1/2}\left(\frac{2\mu Hw}{\bar{w}}\right), \quad (26)$$

which, in its normalized form, yields Equation (18). The  $\eta$ - $\mu$  envelope probability density function can be written from Equation (26) as

$$\hat{r}f_R(r) = \frac{4\sqrt{\pi}\mu^{\mu+1/2}h^\mu}{\Gamma(\mu)H^{\mu-1/2}} \left( \frac{r}{\hat{r}} \right)^{2\mu} \exp\left[-2\mu h \left( \frac{r}{\hat{r}} \right)^2\right] I_{\mu-1/2}\left[2\mu H \left( \frac{r}{\hat{r}} \right)^2\right], \quad (27)$$

which, in its normalized version, yields Equation (17).

Now, consider the physical model for the  $\eta$ - $\mu$  distribution Format 2. The envelope,  $R$ , can be written in terms of the in-phase and quadrature components of the fading signal as in Equation (22), where  $X_i$  and  $Y_i$  are mutually correlated Gaussian processes with  $E(X_i) = E(Y_i) = 0$ ,  $E(X_i^2) = E(Y_i^2) = \sigma^2$ , and  $n$  is the number of clusters of multipath. Defining the correlation coefficient between the in-phase and quadrature components to be  $\eta = E(X_i Y_i)/\sigma^2$  and carrying out the standard procedure to find the probability density function, as required, we arrive at exactly the same formulations as shown for Format 1, the difference being that now  $-1 < \eta < 1$ , and, consequently,  $h$  and  $H$  are defined accordingly. Alternatively, one may depart from the correlated variates  $X_i$  and  $Y_i$  as defined previously, and make a rotation of the axis so as to arrive at independent in-phase and quadrature variates having variances respectively equal to  $\sigma_{X_i}^2 = (1-\eta)\sigma^2$  and  $\sigma_{Y_i}^2 = (1+\eta)\sigma^2$ . Again, following the standard procedure, the required distribution is found as before.

### 3.3 The $\eta$ - $\mu$ Distribution and the Other Fading Distributions

The  $\eta$ - $\mu$  distribution is a general fading distribution that includes the Hoyt (Nakagami- $q$ ), the One-Sided Gaussian, the Rayleigh, and, more generally, the Nakagami- $m$  distributions as special cases.

#### 3.3.1 Hoyt, Nakagami- $q$ , One-Sided Gaussian, and Rayleigh

The Hoyt (or Nakagami- $q$ ) distribution can be obtained from the  $\eta$ - $\mu$  distribution in an exact manner by setting  $\mu = 0.5$ . In this case, the Hoyt (or Nakagami- $q$ ) parameter is given by  $b = \frac{1-\eta}{1+\eta}$

(or  $q^2 = \eta$ ) in Format 1, or  $b = -\eta$  (or  $q^2 = \frac{1-\eta}{1+\eta}$ ) in Format 2.

From these, the One-Sided Gaussian distribution is obtained for  $\eta \rightarrow 0$  or  $\eta \rightarrow \infty$  in Format 1, or  $\eta \rightarrow \pm 1$  in Format 2. In the same way, the Rayleigh distribution is obtained in an exact manner for  $\mu = 0.5$  and by setting  $\eta = 1$  in Format 1 or  $\eta = 0$  in Format 2.

#### 3.3.2 Nakagami- $m$ , Rayleigh, and One-Sided Gaussian

The Nakagami- $m$  distribution can be obtained in an exact manner from the  $\eta$ - $\mu$  distribution for  $\mu = m$  and  $\eta \rightarrow 0$  or  $\eta \rightarrow \infty$  in Format 1 or  $\eta \rightarrow \pm 1$  in Format 2. In the same way, it can be attained by setting  $\mu = m/2$  and  $\eta \rightarrow 1$  in Format 1 or  $\eta \rightarrow 0$  in Format 2. These cases are explored in Appendix A. Through the Nakagami- $m$  distribution, the One-Sided Gaussian is obtained for  $m = 0.5$ , whereas the Rayleigh distributions is obtained for  $m = 1$ .



### 3.4 Estimators for the Parameters

Moment-based estimators for the parameters  $\eta$  and  $\mu$  can be obtained as follows. We shall initially introduce these estimators for Format 1. Replacing Equation (25) in Equation (21) for  $j = 6$ , and after algebraic manipulations, two sets for  $\eta$  are found:

$$\eta_{1,2} = \eta_{3,4}^{-1} = \frac{\sqrt{2c} + \sqrt{3-2c \pm \sqrt{9-8c}}}{\sqrt{2c} - \sqrt{3-2c \pm \sqrt{9-8c}}} \quad (28)$$

with

$$c = \frac{E(\rho^6) - 3E(\rho^4) + 2}{2[E(\rho^4) - 1]^2}$$

As already mentioned,  $\eta$  and  $\eta^{-1}$  lead to the same envelope (power) density. Therefore, one may use either  $\eta_1$  or  $\eta_3^{-1}$  without distinction, and either  $\eta_2$  or  $\eta_4^{-1}$  without distinction. Note, however, that there is an ambiguity in this estimation, i.e.,  $\eta_1$  (or equivalently,  $\eta_3^{-1}$ ) and  $\eta_2$  (or equivalently,  $\eta_4^{-1}$ ). Therefore, from Equation (25), two corresponding parameters,  $\mu_1$  and  $\mu_2$ , are estimated. Now, in order to decide which pair of estimators ( $\eta_1, \mu_1$ ) or ( $\eta_2, \mu_2$ ) is the appropriate pair, another moment of the envelope must be used, e.g., the first moment. The aim is to compare the first moment,  $E(D)$ , of the normalized envelope obtained from the data with that of  $E(P)$  calculated from Equation (21) for each pair ( $\eta_1, \mu_1$ ) and ( $\eta_2, \mu_2$ ), and to then choose the pair providing the smallest absolute deviation,  $|E(D) - E(P)|$ . Of course, if  $D$  follows the  $\eta - \mu$  distribution, then the smallest deviation is zero. As for Format 2, by carrying out the same procedure – or, alternatively, by using the appropriate conversion formula, as given previously – and making the appropriate simplifications, we find

$$\eta_{1,2} = -\eta_{3,4} = \sqrt{\frac{3 \pm \sqrt{9-8c}}{2c}} - 1. \quad (29)$$

### 3.5 Application of the $\eta - \mu$ Distribution

As implied in its name, the  $\eta - \mu$  distribution is based on two parameters,  $\eta$  and  $\mu$ . Therefore, its use requires the estimation of these parameters. Alternatively, in order to use it the following procedure may be carried out. From Equation (25), it can be seen that the two parameters  $\eta$  and  $\mu$  can be expressed in terms of the normalized variance of the power of the fading signal, which is usually defined as  $m$ . In other words,

$$m = 2\mu \left[ 1 + \left( \frac{H}{h} \right)^2 \right]^{-1}. \quad (30)$$

For a given  $m$ , the parameters  $\eta$  and  $\mu$  are chosen that yield the best fit. On the other hand, note that because  $-1 \leq H/h \leq 1$  for a given  $m$ , the parameter  $\mu$  will lie within the range  $m/2$  and  $m$ . Therefore, for a given  $m$ ,

$$m/2 \leq \mu \leq m. \quad (31)$$

The parameter  $\mu$  is then chosen within the range of Equation (31). Given that  $\mu$  has been chosen, then  $\eta$  is calculated from Equation (30) as

$$\frac{H}{h} = \sqrt{\frac{2\mu}{m} - 1}. \quad (32)$$

### 3.6 The $\eta - \mu$ Distribution for a Fixed $m$

Equation (30) shows that for a given  $m$ , an infinite number of curves of the  $\eta - \mu$  distribution can be found that present the same Nakagami parameter, conditioned on the fact that the constraints of Equations (31) and (32) are satisfied. The Nakagami curve is obtained for  $H/h \rightarrow 0$ , in which case  $\mu = m/2$ , or, equivalently, for  $H/h \rightarrow \pm 1$ , in which case  $\mu = m$ . The Hoyt distribution is obtained for  $\mu = 0.5$ . Figures 7 and 8 respectively depict a sample

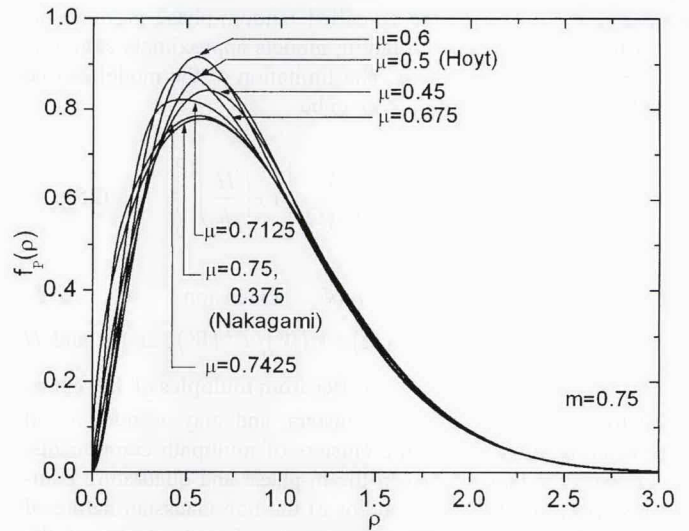


Figure 7. The  $\eta - \mu$  probability density function for the same Nakagami parameter  $m$  ( $m = 0.75$ ).

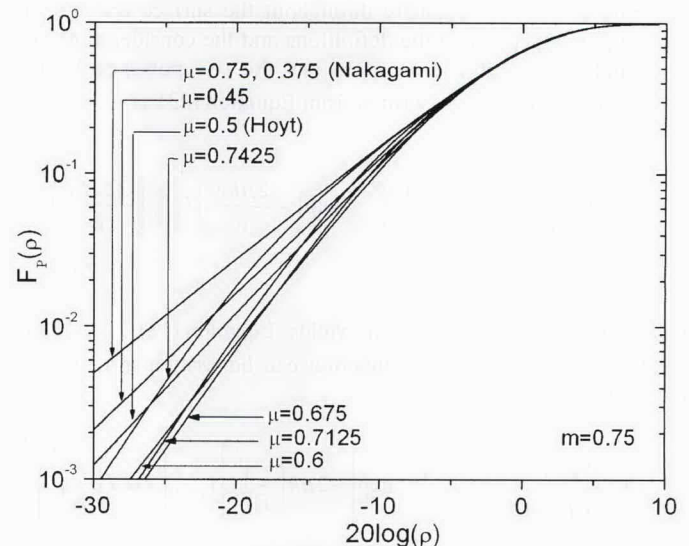


Figure 8. The  $\eta - \mu$  probability distribution function for the same Nakagami parameter  $m$  ( $m = 0.75$ ).

of the various shapes of the  $\eta$ - $\mu$  probability density function,  $f_p(\rho)$ , and the probability distribution function,  $F_p(\rho)$ , as a function of the normalized envelope,  $\rho$ , for the same Nakagami parameter,  $m = 0.75$ . It can be seen that although the normalized variance (parameter  $m$ ) is kept constant for each figure, the curves are substantially different from each other. This is particularly noticeable for the distribution function, in which case the lower tail of the distribution may yield differences in the probability of some orders of magnitude.

### 3.7 Sum of $\eta$ - $\mu$ Variates

From the definition of the  $\eta$ - $\mu$  distribution, it is easy to see that the sum of  $M$  independent identically distributed  $\eta$ - $\mu$  power variates is also  $\eta$ - $\mu$  distributed, but with parameters  $\eta$  and  $\mu M$ . Now, the sum of  $M$  independent identically distributed  $\eta$ - $\mu$  envelope variates may be well approximated by another  $\eta$ - $\mu$  distribution, the parameters of which are estimated accordingly. The procedure in order to obtain these parameters follows that given in [17], where it was shown that the  $\eta$ - $\mu$  distribution can be used in order to approximate the distribution of the sum of Hoyt (Nakagami- $q$  and also Nakagami- $m$ ) variates. In [17], it was demonstrated that exact and approximate curves were almost indistinguishable from each other. The distribution of the sum of independent non-identically-distributed  $\eta$ - $\mu$  variates (power or envelope) may also be approximated by a  $\eta$ - $\mu$  distribution, although in this case, the resulting curves are not as accurate as for the independent identically distributed case.

## 4. The $\kappa$ - $\mu$ Distribution and The $\eta$ - $\mu$ Distribution

In the  $F_p(\rho) \times \rho$  plane using a logarithmic scale (the fading plane), given a fixed Nakagami parameter,  $m$ , the curves belonging to the  $\kappa$ - $\mu$  distribution are all found above the Nakagami- $m$  curve, whereas those belonging to the  $\eta$ - $\mu$  distribution are all encountered below the Nakagami- $m$  curve. A sample of these is illustrated in Figures 4 and 8 for the respective distributions. As already mentioned, the Nakagami- $m$  curve is included in both distributions. Generally speaking, the Nakagami- $m$  distribution can be thought of as a mean distribution, which divides the fading plane into two: the upper plane, described by the  $\kappa$ - $\mu$  distribution, and the lower plane, described by the  $\eta$ - $\mu$  distribution. In Figure 9, such a feature is illustrated for  $m = 1.25$ . This is a very interesting attribute, which can be used in order to choose the best distribution to fit experimental data, as explained next. For a given set of data, the Nakagami parameter  $m$  is calculated, and the experimental data are plotted in the fading plane. In case these data are found above the Nakagami- $m$  curve, then the best distribution to fit these data is the  $\kappa$ - $\mu$  distribution; otherwise, the best distribution is the  $\eta$ - $\mu$  distribution. Note that the versatility provided by the use of two parameters renders these two distributions suited for applications in which other distributions fail to yield a good fit, particularly for low values of the fading envelope. The question raised in [4] concerning the inadequacy of the tails of some distributions to fit experimental data is notably less critical in these distributions.

## 5. Validation Through Field Measurements

A series of field trials was conducted in downtown Campinas, Brazil, and at the Unicamp university campus, in order to investigate the short-term statistics of the fading signal. Basically, the reception setup consisted of a vertically polarized omnidirectional antenna, a low-noise amplifier, a spectrum analyzer, a data-acquisition apparatus, a notebook computer, and a distance transducer. A forward control channel at 870.9 MHz of an analog cellular system in downtown Campinas, and a CW signal at 1.8 GHz at the university campus were used. The spectrum analyzer was set to zero span and centered at the required frequency, and its video output was used as the input of the data-acquisition and processing equipment. The local mean was estimated through the moving-average method, with the average being conveniently taken over samples symmetrically adjacent to every point, a procedure widely reported in the literature [18]. The practice used in

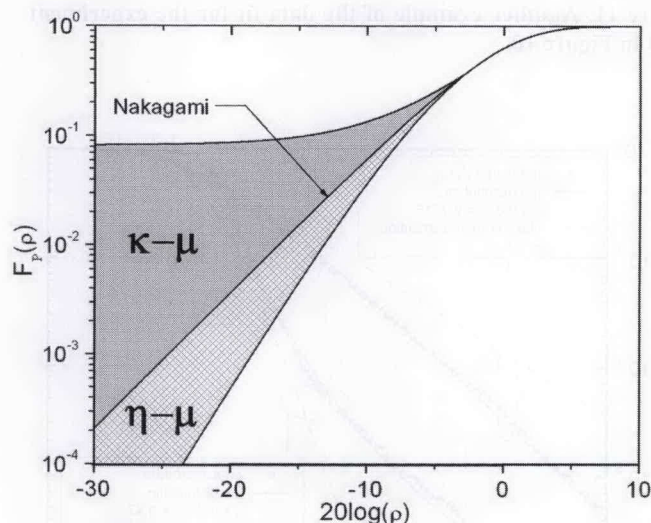


Figure 9. The  $\kappa$ - $\mu$  distribution and the  $\eta$ - $\mu$  distribution for the same Nakagami parameter  $m$  ( $m = 1.25$ ).

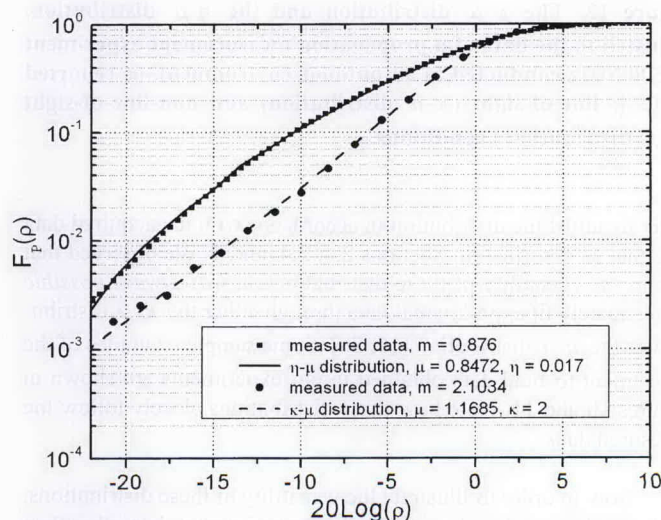


Figure 10. The  $\kappa$ - $\mu$  distribution and the  $\eta$ - $\mu$  distribution, adjusted to the data of a propagation measurement experiment at 1.8 GHz, conducted in an indoor (line of sight -  $\kappa$ - $\mu$  distribution) as well as an outdoor (non-line-of-sight) environment at the University of Campinas.

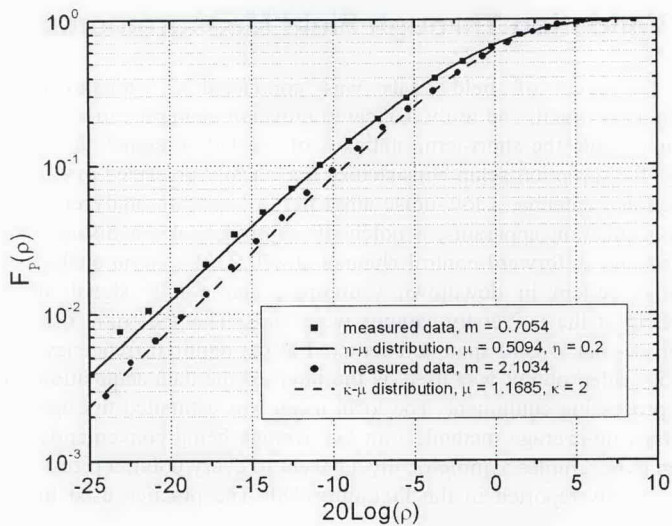


Figure 11. Another example of the data fit for the experiment cited in Figure 10.

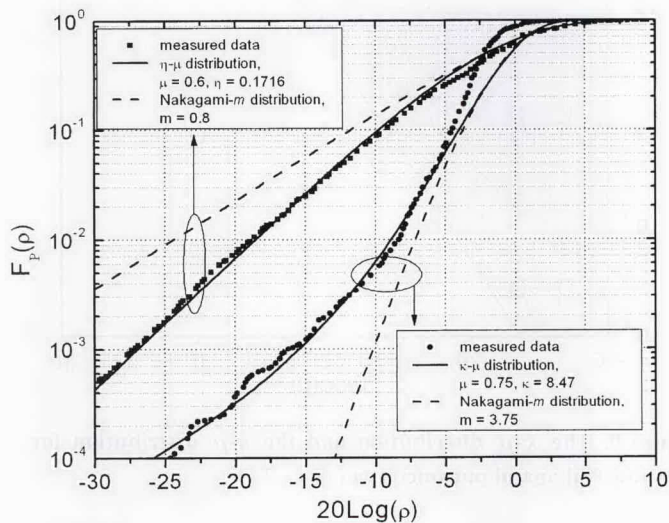


Figure 12. The  $\kappa$ - $\mu$  distribution and the  $\eta$ - $\mu$  distribution, adjusted to the data of a propagation measurement experiment at 500 MHz conducted in an outdoor environment, as reported in [21]: line-of-sight ( $\kappa$ - $\mu$  distribution) and non-line-of-sight ( $\eta$ - $\mu$  distribution) conditions.

order to adjust the distribution in accordance with the acquired data was that as described in Sections 2.4, 3.4, and 4. We observed that due to the versatility of these distributions, it was *always possible* to adequately fit experimental data through either the  $\kappa$ - $\mu$  distribution or the  $\eta$ - $\mu$  distribution [19, 20]. Some sample examples of the adjustment to field data obtained in our experiments are shown in Figures 10 and 11. Note how these distributions closely follow the measured data.

Now in order to illustrate the versatility of these distributions, in this paper we also show their fit to experimental data other than those obtained by the author. We then turn our attention to [21], in which a propagation measurement experiment at 500 MHz conducted in an outdoor environment was reported. In Figure 9 of [21], the authors plotted the experimental data and the Rayleigh curve. It could clearly be seen that the Rayleigh adjustment was

rather poor. We then carefully extracted experimental points from these curves and used the investigated distributions to adjust them, and this is shown in Figures 12 and 13. Note how the fit attained with these distributions was indeed excellent.

Finally, we explored [18], in which a propagation measurement experiment at 10 GHz, conducted in an indoor environment, was reported. In Figure 4 of [18], where a logarithmic scale was used, it could be seen that the fit provided by Rayleigh and Rice distributions to the experimental data was rather poor. Still in [18], the same set of data was then fitted to the Nakagami- $m$  distribution, and this is shown in Figure 5 of [18]. The fit was better in this case, but a linear scale was used, although the linear scale was not suitable for highlighting the behavior of the tail of the distribution. In order to adjust the  $\kappa$ - $\mu$  distribution or the  $\eta$ - $\mu$  distribution to the data of [18], these data were carefully extracted from Figure 4 of [18]. By then using the respective Nakagami parameter,  $m$ , for

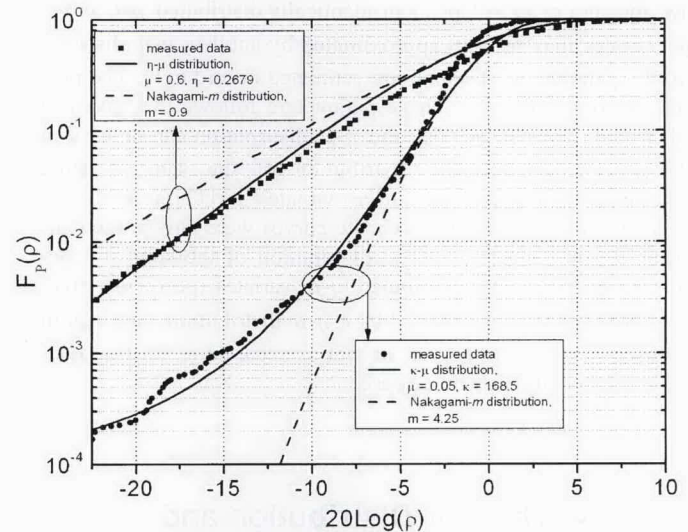


Figure 13. Another example of the data fit for the experiment cited in Figure 12.

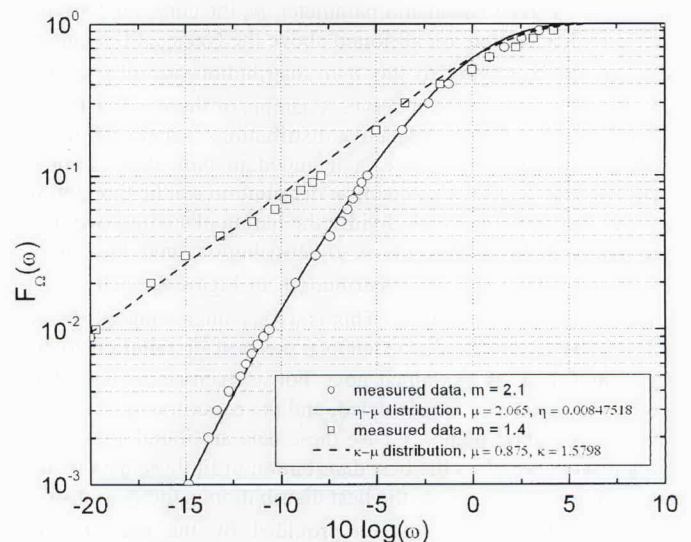


Figure 14: The  $\kappa$ - $\mu$  distribution and the  $\eta$ - $\mu$  distribution adjusted to the data of a propagation measurement experiment at 10 GHz conducted in an indoor environment, as reported in [18].

each set of data – the same parameter as reported in [18] – the parameters of the distributions under test were adjusted to yield the best fit for each fixed  $m$ . In all of the cases, the fit given by the  $\kappa$ - $\mu$  distribution or the  $\eta$ - $\mu$  distribution was better than that given by the Rayleigh, Rice, Nakagami, or Weibull distributions. Figure 14 shows this for the case in which  $m = 2.1$  (Figure 4b and Figure 5c of [18]) and for  $m = 1.4$  (Figure 4c and Figure 5a of [18]).

## 6. Conclusions

This paper presented two general fading distributions: the  $\kappa$ - $\mu$  distribution and the  $\eta$ - $\mu$  distribution. The  $\kappa$ - $\mu$  distribution includes the Rice (and therefore, the Rayleigh) and the Nakagami- $m$  (and therefore, the Rayleigh and the One-Sided Gaussian) distributions as special cases. The  $\eta$ - $\mu$  distribution includes the Hoyt (or Nakagami- $q$ ) (and therefore, the Rayleigh and the One-Sided Gaussian) and the Nakagami- $m$  (and therefore, the Rayleigh and the One-Sided Gaussian) distributions as special cases. Note that the Nakagami- $m$  distribution is included in both distributions, and it defines a “border” between the two distributions in the fading plane. Generally speaking, the Nakagami- $m$  distribution can be thought of as a mean distribution with respect to the  $\kappa$ - $\mu$  distribution and the  $\eta$ - $\mu$  distribution. Because these distributions are more flexible than the other fading distributions, they can yield better fits to experimental data. This has been observed in several field-measurement campaigns, carried out both by the author of this paper together with his team, as well as by other researchers.

## 7. Acknowledgements

The author is in debt to a number of people who in one way or another have lent their help to accomplishing this work: Prof. Max Gerken (in memoriam), Prof. Paulo Cardieri, Prof. Sandro Adriano Fasolo, Dr. Álvaro Augusto Machado de Medeiros, Dr. Cláudio Rafael Cunha Monteiro da Silva, Dr. Ernesto Luiz Andrade Neto, Dr. Gustavo Fraindenraich, Dr. José Cândido Silveira Santos Filho, Daniel Benevides da Costa, Denilson Oliveira Figueiredo, Hermano Barros Tercius, Jamil Ribeiro Antônio, José Ricardo Mendes, Maurício Sol de Castro, Rausley Adriano Amaral de Souza, Renan Sthel Duque, and Ugo Silva Dias.

## 8. Appendix A: The Distributions for Limiting Values of the Parameters

This appendix obtains the expressions of the distributions for the cases in which the simple substitution of the parameters in the formulas leads to indeterminacy.

### 8.1 The $\kappa$ - $\mu$ Distribution for $\kappa \rightarrow 0$

For small arguments of the Bessel function, the relation  $I_{\nu-1}(z) \approx (z/2)^{\nu-1}/\Gamma(\nu)$  holds [14, Equation 9.6.7]. Using this in Equation (1), and after some algebraic manipulation,

$$f_P(\rho) \approx \frac{2\mu^\mu (1+\kappa)^\mu}{\exp(\mu\kappa)\Gamma(\mu)} \rho^{2\mu-1} \exp[-\mu(1+\kappa)\rho^2]. \quad (33)$$

As  $\kappa \rightarrow 0$ , Equation (33) reduces to

$$f_P(\rho) = \frac{2\mu^\mu}{\Gamma(\mu)} \rho^{2\mu-1} \exp(-\mu\rho^2), \quad (34)$$

which is the Nakagami- $m$  density function for the normalized envelope. In this case, the parameter  $\mu$  coincides with the well-known Nakagami parameter,  $m$ .

### 8.2 The $\kappa$ - $\mu$ Distribution for a Fixed $m$ and $\kappa \rightarrow \infty$ ( $\mu \rightarrow 0$ )

Given a fixed  $m$ , as  $\kappa \rightarrow \infty$  then  $\mu \rightarrow 0$ . Therefore,  $\kappa+1 \approx \kappa$  and  $\mu \pm 1 \approx \pm 1$ . Using these in Equation (1) and knowing that an impulse appears at the origin (observe the trend depicted in Figure 3) and that  $I_{-1}(z) = I_1(z)$ , then

$$f_P(\rho) = \frac{2\mu\kappa^{0.5}}{\kappa^{-0.5}\exp(\mu\kappa)} \exp(-\mu\kappa\rho^2) I_1(2\mu\kappa\rho) + K\delta(\rho), \quad (35)$$

where  $K$  is a normalization constant to be determined. In the same way, we have that  $m/\mu \gg 1$ . Using this in Equation (15), then  $\kappa\mu \approx 2m$ . With such a result replaced in Equation (35),

$$f_P(\rho) = \frac{4m}{\exp(2m)} \exp(-2m\rho^2) I_1(4m\rho) + C\delta(\rho). \quad (36)$$

The normalization constant,  $C$ , is determined so that Equation (36) is a probability density function (i.e.,  $\int_0^\infty f_P(\rho) d\rho = 1$ ). Using the result of [22, Equation 6.618-4], such a constant can be found in an exact fashion to be  $C = 1 - \frac{\sqrt{2m\pi}}{\exp(m)} I_{0.5}(m)$ . This result is used in Equation (36) to yield Equation (16).

### 8.3 The $\eta$ - $\mu$ Distribution for $H \rightarrow 0$

This corresponds to the case in which  $\eta \rightarrow 1$  in Format 1 or  $\eta \rightarrow 0$  in Format 2. For small arguments of the Bessel function, the relation  $I_{\nu-1}(z) \approx (z/2)^{\nu-1}/\Gamma(\nu)$  holds [14, Equation 9.6.7]. Using this in Equation (17) and knowing that in this case  $h = 1$ , and after algebraic manipulations,

$$f_P(\rho) \approx \frac{4\sqrt{\pi}\mu^{2\mu}}{\Gamma(\mu)\Gamma(\mu+0.5)} \rho^{4\mu-1} \exp(-2\mu\rho^2). \quad (37)$$

Making use of  $2^{2\nu-0.5}\Gamma(\nu)\Gamma(\nu+0.5) = \sqrt{2\pi}\Gamma(2\nu)$  [14, Equation 6.1.18] in Equation (37), then

$$f_P(\rho) = \frac{2(2\mu)^{2\mu}}{\Gamma(2\mu)} \rho^{2(2\mu)-1} \exp(-2\mu\rho^2), \quad (38)$$

which is the Nakagami- $m$  density function for the normalized envelope. In this case, the parameter  $\mu$  and the Nakagami parameter  $m$  are related to each other by  $m = 2\mu$ .

## 8.4 The $\eta$ - $\mu$ Distribution for $H \rightarrow \pm\infty$

This corresponds to the case in which  $\eta \rightarrow 0$  or  $\eta \rightarrow \infty$  in Format 1, or  $\eta \rightarrow \pm 1$  in Format 2. Assume that  $H > 0$ . For large arguments of the Bessel function, and utilizing the first term of the expansion in [14, Equation 9.7.1], the relation  $I_\nu(z) \approx \frac{\exp(z)}{\sqrt{2\pi z}}$

holds. Using this in Equation (17), and after algebraic manipulations,

$$f_P(\rho) \approx \frac{2\mu^\mu}{\Gamma(\mu)} \left(\frac{h}{H}\right)^\mu \rho^{2\mu-1} \exp[-2\mu(h-H)\rho^2]. \quad (39)$$

For those *specific conditions*,  $h/H=1$  and  $h-H=0.5$ . Then, Equation (39) reduces to

$$f_P(\rho) = \frac{2\mu^\mu}{\Gamma(\mu)} \rho^{2\mu-1} \exp(-\mu\rho^2), \quad (40)$$

which is the Nakagami- $m$  density function for the normalized envelope. In this case, the parameter  $\mu$  coincides with the well-known Nakagami parameter  $m$ . For  $H < 0$ , we use the property  $I_\nu(-z) = (-1)^\nu I_\nu(z)$  and proceed to obtain the same result.

## 9. Appendix B: The Extended Forms of the $\eta$ - $\mu$ Distribution

In this appendix, we write the distribution directly in terms of its parameters.

### 9.1 The $\eta$ - $\mu$ Distribution: Format 1

The  $\eta$ - $\mu$  probability density function,  $f_P(\rho)$ , is written as

$$f_P(\rho) = \frac{2\sqrt{\pi}(1+\eta)^{\mu+\frac{1}{2}} \mu^{\mu+\frac{1}{2}} \rho^{2\mu}}{\sqrt{\eta}(1-\eta)^{\mu-\frac{1}{2}} \Gamma(\mu)} \exp\left[-\frac{\mu(1+\eta)^2 \rho^2}{2\eta}\right] I_{\mu-\frac{1}{2}}\left[\frac{\mu(1-\eta^2)\rho^2}{2\eta}\right], \quad (41)$$

with  $\mu = \frac{1}{V(P^2)} \frac{1+\eta^2}{(1+\eta)^2}$ . The  $\eta$ - $\mu$  probability distribution function,  $F_P(\rho)$ , is written as

$$F_P(\rho) = 1 - Y_\mu\left(\frac{1-\eta}{1+\eta}, (1+\eta)\sqrt{\frac{\mu}{2\eta}}\rho\right). \quad (42)$$

The  $j$ th moment  $E(P^j)$  of  $P$  is obtained as

$$E(P^j) = \frac{2^{2\mu+j/2} \Gamma(2\mu+j/2)}{(2+\eta^{-1}+\eta)^{\mu+j/2} \mu^{j/2} \Gamma(2\mu)} {}_2F_1\left[\mu+\frac{j}{4}+\frac{1}{2}, \mu+\frac{j}{4}; \mu+\frac{1}{2}; \left(\frac{1-\eta}{1+\eta}\right)^2\right]. \quad (43)$$

## 9.2 The $\eta$ - $\mu$ Distribution: Format 2

The  $\eta$ - $\mu$  probability density function,  $f_P(\rho)$ , is written as

$$f_P(\rho) = \frac{4\sqrt{\pi}\mu^{\mu+\frac{1}{2}} \rho^{2\mu}}{\eta^{\mu-\frac{1}{2}} \sqrt{1-\eta^2} \Gamma(\mu)} \exp\left(-\frac{2\mu\rho^2}{1-\eta^2}\right) I_{\mu-\frac{1}{2}}\left(\frac{2\eta\mu\rho^2}{1-\eta^2}\right), \quad (44)$$

with  $\mu = \frac{1}{V(P)} \frac{1+\eta^2}{2}$ . The  $\eta$ - $\mu$  probability distribution function,  $F_P(\rho)$ , is written as

$$F_P(\rho) = 1 - Y_\mu\left(\eta, \sqrt{\frac{2\mu}{1-\eta^2}}\rho\right). \quad (45)$$

The  $j$ th moment,  $E(P^j)$ , of  $P$  is obtained as

$$E(P^j) = \frac{(1-\eta^2)^{\mu+j/2} \Gamma(2\mu+j/2)}{(2\mu)^{j/2} \Gamma(2\mu)} {}_2F_1\left(\mu+\frac{j}{4}+\frac{1}{2}, \mu+\frac{j}{4}; \mu+\frac{1}{2}; \eta^2\right). \quad (46)$$

## 10. Appendix C: Some Properties of the Function $Y_\nu(a, b)$

In this appendix,  $Y_\nu(a, b)$  is written in terms of the incomplete gamma function,  $\Gamma(\bullet, \bullet)$  [14, Equation 6.5.3], for the limiting values of the parameter  $a$ .

### 10.1 $Y_\nu(a, b)$ for $a$ Approaching Zero

Using the same approximations as in Section 8.3, we arrive at

$$Y_\nu(a, b) \approx \frac{\Gamma(2\nu, b^2)}{\Gamma(2\nu)}. \quad (47)$$

### 10.2 $Y_\nu(a, b)$ for $a$ Approaching One

Using the same approximations as in Section 8.4, we arrive at

$$Y_\nu(a, b) \approx \frac{\Gamma[\nu, (1-a)b^2]}{\Gamma(\nu)} \quad (48)$$

## 11. References

1. W. R. Braun and U. Dersch, "A Physical Mobile Radio Channel Model," *IEEE Trans. Veh. Technol.*, **40**, 2, May 1991, pp. 472-482.
2. H. Suzuki, "A Statistical Model for Urban Radio Propagation," *IEEE Trans. Commun.*, **COM-25**, 7, July 1977, pp. 673-679.
3. J. D. Parsons, *The Mobile Radio Channel, Second Edition*, New York, John Wiley & Sons, 2000.
4. S. Stein, "Fading Channel Issues in System Engineering," *IEEE J. Selected Areas in Commun.*, **5**, 2, February 1987, pp. 68-69.
5. M. Nakagami and M. Nishio, "Generalized Forms of the Basic Distributions," *Ann. Conv. Record*, Japan, 1954.
6. M. Nakagami, "The m-Distribution – A General Formula of Intensity Distribution of Rapid Fading," in W. C. Hoffman (ed.), *Statistical Methods in Radio Wave Propagation*, Elmsford, NY, Pergamon, 1960.
7. H. Cramer, *Mathematical Methods of Statistics*, Princeton, NJ, Princeton University Press, 1946.
8. J. I. Marcum, "A Statistical Theory of Target Detection by Pulsed Radar," Project RAND, Douglas Aircraft Company, Inc., RA-15061, December 1, 1947.
9. K. A. Norton, L. E. Vogler, W. V. Mansfield, and P. J. Short, "The Probability Distribution of the Amplitude of a Constant Vector Plus a Rayleigh Distributed Vector," *Proc. IRE*, **43**, October 1955, pp. 1354-1361.
10. A. T. McKay, "A Bessel Function Distribution," *Biometrika*, **24**, 1/2, May 1932, pp. 39-44.
11. M. D. Yacoub, "The  $\eta-\mu$  Distribution: A General Fading Distribution," IEEE Boston Fall Vehicular Technology Conference 2000, Boston, USA, September 2000.
12. M. D. Yacoub, "The  $\kappa-\mu$  Distribution: A General Fading Distribution," IEEE Atlantic City Fall Vehicular Technology Conference 2001, Atlantic City, USA, October 2001.
13. G. Fraidenraich and M. D. Yacoub, "The  $\lambda-\mu$  General Fading Distribution," SBMO/IEEE International Microwave and Optoelectronics Conference, IMOC2003, Foz do Iguaçu, Brazil, 2003.
14. M. Abramowitz and I. A. Stegun, *Handbook of Mathematical Functions*, Washington, DC, US Dept. of Commerce, National Bureau of Standards, 1972.
15. H. Asplund, A. F. Molisch, M. Steinbauer, and N. B. Mehta, "Clustering of Scatterers in Mobile Radio Channels – Evaluation and Modeling in the COST259 Directional Channel Model, IEEE International Conference on Communications," IEEE International Conference on Communications, ICC 2002, New York, April-May 2002.
16. J. C. S. Santos Filho and M. D. Yacoub, "Highly Accurate  $\kappa-\mu$  Approximation to Sum of M Independent Non-Identical Ricean Variates," *IEE Electronics Letters*, **41**, 6, March 2005, pp. 338-339.
17. J. C. S. Santos Filho and M. D. Yacoub, "Highly Accurate  $\eta-\mu$  Approximation to Sum of M Independent Non-Identical Hoyt Variates," *IEEE Antennas and Wireless Propagation Letters*, **4**, December 2005, pp. 436-438.
18. A. F. Abouraddy and S. M. Elnoubi, "Statistical Modeling of the Indoor Radio Channel at 10 GHz Through Propagation Measurements – Part I: Narrow-Band Measurements and Modeling," *IEEE Trans. Veh. Technol.*, **49**, 5, September 2000, pp. 1491-1507.
19. F. C. Martins, H. B. Tercius, and M. D. Yacoub, "Validating the  $\kappa-\mu$  and the  $\eta-\mu$  Distribution," International Workshop on Telecommunications, IWT 2004, Santa Rita do Sapucaí, MG, Brazil, August 2004.
20. F. C. Martins, H. B. Tercius, and M. D. Yacoub, "Narrowband Measurement at 1800 MHz and the  $\kappa-\mu$  and  $\eta-\mu$  Fading Distributions," XXI Brazilian Telecommunication Symposium, SBT'04, Belém, PA, September 2004.
21. B. R. Davis and R. E. Bogner, "Propagation at 500 MHz for Mobile Radio," *IEE Proceedings*, **132**, F, 5, August 1985.
22. I. S. Gradshteyn and I. M. Ryzhik, *Table of Integrals, Series, and Products, Fourth Edition*, New York, Academic Press, 1965.